J Mol Model (2013) 19:3481–3489
DOI 10.1007/s00894-013-1870-4

ORIGINAL PAPER

Thermal, electronic and ductile properties of lead-chalcogenides under pressure

Dinesh C. Gupta · Idris Hamid Bhat

Received: 7 March 2013 / Accepted: 30 April 2013 / Published online: 25 May 2013

Abstract Fully relativistic pseudo-potential ab-initio calculations have been performed to investigate the high pressure phase transition, elastic and electronic properties of lead-chalcogenides including the less known lead polonium. The calculated ground state parameters, for the rock-salt structure show good agreement with the experimental data. PbS, PbSe, PbTe and PbPo undergo a first-order phase transition from rock-salt to CsCl structure at 19.4, 15.5, 11.5 and 7.3 GPa, respectively. The elastic properties have also been calculated. The calculations successfully predicted the location of the band gap at *L*-point of Brillouin zone and the band gap for each material at ambient pressure. It is observed that unlike other lead-chalcogenides, PbPo is semi-metal at ambient pressure. The pressure variation of the energy gap indicates that these materials metalize under pressure. The electronic structures of these materials have been computed in parent as well as in high pressure B2 phase.

Keywords Elastic properties · Electronic structure · Lead-chalcogenides · Narrow band-gap semiconductors · Phase transition

Introduction

Lead chalcogenides (PbX : X=S, Se, Te, Po) exhibit a series of electronic structure anomalies relative to other semiconductors (II–VI) that have attracted experimental and theoretical attention due to the pressure and temperature dependence of the energy gap [1–3]. These materials possess interesting structural, mechanical, optoelectronic and electronic properties [4] which make them better candidates for industrial and technological applications [5, 6]. Synchrotron radiation and XRD studies on these compounds show that they crystallize in NaCl or rock-salt (RS) structure and their lattice parameter '*a*' increases with increasing anion size. Lead chalcogenides share many physical and chemical properties in common and are isostructural [7]. These materials exhibit direct narrow band gap, which gives an opportunity to use interband transition in detection or emission of radiation. This feature gives much freedom in design of optoelectronic structures and makes them simple to manufacture. Moreover, lead chalcogenides have a lower Auger recombination rate than GaAs based semiconductors [6]. The spectral detectivities of III–V and IV–VI materials are comparable [8, 9]. Therefore, IV–VI semiconductor devices are of considerable interest for investigation of their radiation emission and detection properties.

Under high pressure, PbS, PbSe, and PbTe were observed to transform into the eightfold-coordinated CsCl structure at pressures of 25.3, 18.76, and 15.43 GPa [10–12], respectively. Numerous theoretical calculations have been performed to study the pressure-induced structural transformations, electronic, elastic and optical properties of PbS, PbSe, and PbTe compounds using density functional calculations [10–14] and potential models [15]. However, a very scant amount of attention has been devoted to study the theoretical computation of energy band structure, phase transition and various physical properties of these materials, particularly less studied compound PbPo at both normal as well as high pressures.

A common phase transition sequence (RS→CsCl) is expected in PbPo with pressure below that of PbTe. Bencherif et al. [16] have theoretically predicted RS→CsCl transition in PbPo at 8.5 GPa by generalized gradient approximation (GGA) using both full-potential linearized augmented plane wave (FP-LAPW) and plane wave pseudo-potential methods. However, they have not computed detailed properties of PbPo in high pressure phase.

D. C. Gupta (✉) · I. H. Bhat
Condensed Matter Theory Group, School of Studies in Physics, Jiwaji University, Gwalior 474 011, India
e-mail: sosfizix@yahoo.co.in

D. C. Gupta
e-mail: sosfizix@gmail.com

I. H. Bhat
e-mail: idu.idris@gmail.com

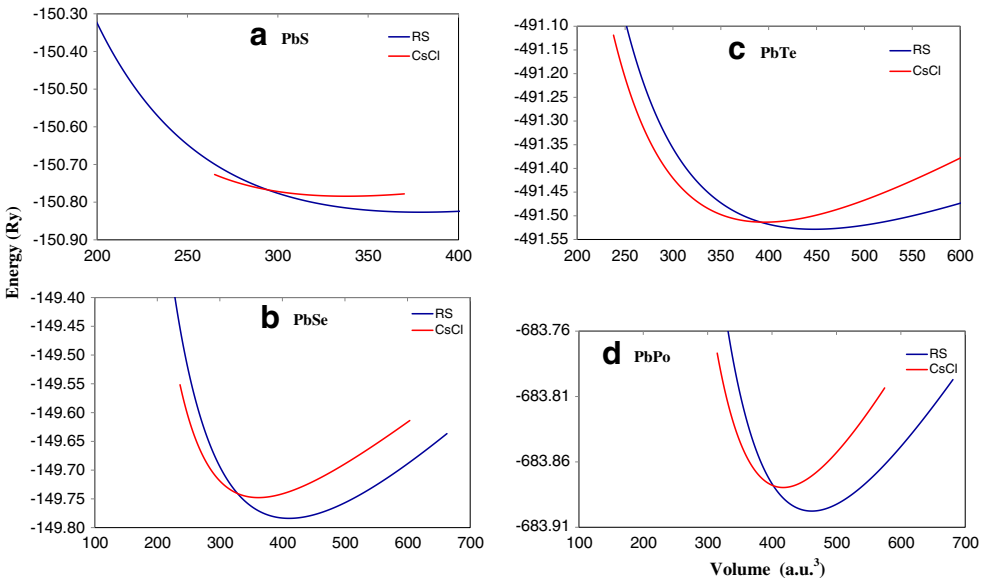

Fig. 1 Energy vs. volume plots for Pb-chalcogenides

The aim of the present work is to perform a combined study of the electronic, structural, phase transition and mechanical properties of lead-chalcogenides in parent (B1) as well as in high pressure (B2) phase using OpenMX code [17, 18]. Here, we have mainly concentrated on the study of a variety of properties of high pressure phase of PbPo which have not yet been reported. A brief description of the computational method will be presented in the next section. In section Results and discussion, we present the main calculated results and discuss them in the light of available data. Finally, a summary is given in section Conclusions.

Computational methods

The calculations have been performed using Ceperly-Alder [19] local density approximation (LDA) exchange-correlation functional used in OpenMX package [20] based on DFT. ADPACK [20] is used to generate fully relativistic pseudo-potentials with demanded number of valence electrons. For all the systems, the pseudo-potentials have been calculated using Troullier-Martins algorithm with Kleinmann-Bylander factorization. An input structure file has been created with a different set of parameters for each material. The pseudo-potentials with the primitive basis sets have been considered for Pb, Po, S and Te throughout the calculations of PbS, PbTe and PbPo. However optimized basis sets (s2p2d1 and s2p1d1 for Pb and Se, respectively) have been used for PbSe. The cut-off radii of confinement potentials were set to 8.0 a.u. for Pb and Po and 7.0, 7.5 and 7.5 a.u. for S, Se and Te, respectively. We have used cut-off energy of 100 Ry in every case with 4x4x4, and 3x3x3 k-point grids for PbS and PbTe, respectively and 4x3x3 for both PbSe and PbPo for the Brillouin zone (BZ) summation. The higher cut-off energy of and a denser k-point grid does not lead to distinguishable changes of band energies. The calculations were performed in both B1 and B2 phases for all the

Table 1 Values of the calculated lattice parameter, the bulk modulus and its pressure derivative at equilibrium volume in RS and CsCl phase

	Rock-salt structure			CsCl structure			References
Solids	a (Å)	B_0 (GPa)	B_0'	a (Å)	B_0 (GPa)	B_0'	
PbS	6.078	63.35	3.42	3.686	70.05	4.10	Present work
	5.936	62.8	–	–	–	–	Expt. ref. [21]
	6.012	52.0	4.38	–	–	–	Theory [22]
PbSe	6.243	54.75	3.45	3.770	56.87	4.49	Present work
	6.124	54.1	–	–	–	–	Expt. ref. [21]
	6.226	44.5	3.64	–	–	–	Theory [22]
PbTe	6.426	39.90	4.06	3.836	57.75	3.47	Present work
	6.462	39.8	–	–	–	–	Expt. ref. [21]
	6.582	37.5	4.27	–	–	–	Theory [22]
PbPo	6.493	37.07	3.10	3.954	61.14	4.83	Present work

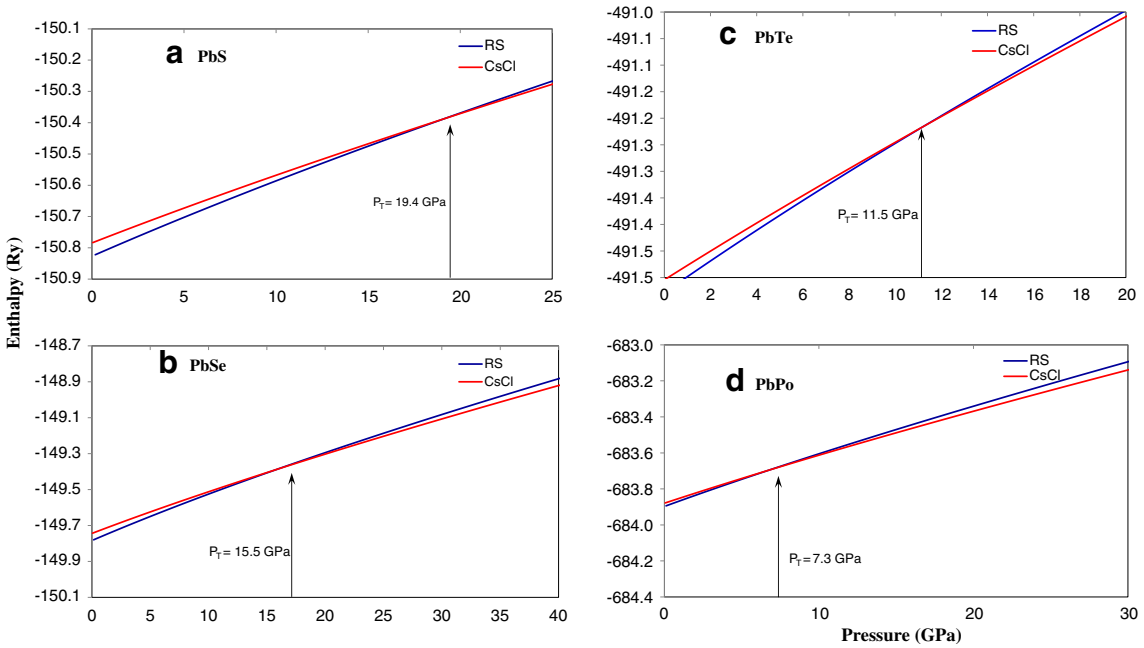

Fig. 2 Enthalpy vs. pressure for Pb-chalcogenides

systems. The lattice constant at equilibrium is obtained computationally by minimizing the total energy as a function of cell volume. The calculations were repeated several times at varying lattice constant to obtain optimized value of the total energy. It was found that the optimized value of the lattice parameter computed in the present case are quite close to the experimental values. The Murnaghan's equation of state which is given as

$$P(V) = \frac{B_0}{B_0'}\left[\left(\frac{V_0}{V}\right)^{B_0'} - 1\right] \tag{1}$$

was fitted to get the values of the equilibrium bulk modulus (B_0) and its first pressure derivative (B_0') which are defined as

$$B_0 = -V\left(\frac{\partial P}{\partial V}\right)_T \quad \text{and} \quad B_0' = \left(\frac{\partial B_0}{\partial P}\right)_T \tag{2}$$

Therefore, B_0 effectively measures the curvature of the energy versus volume curve at the relaxed volume (V=0).

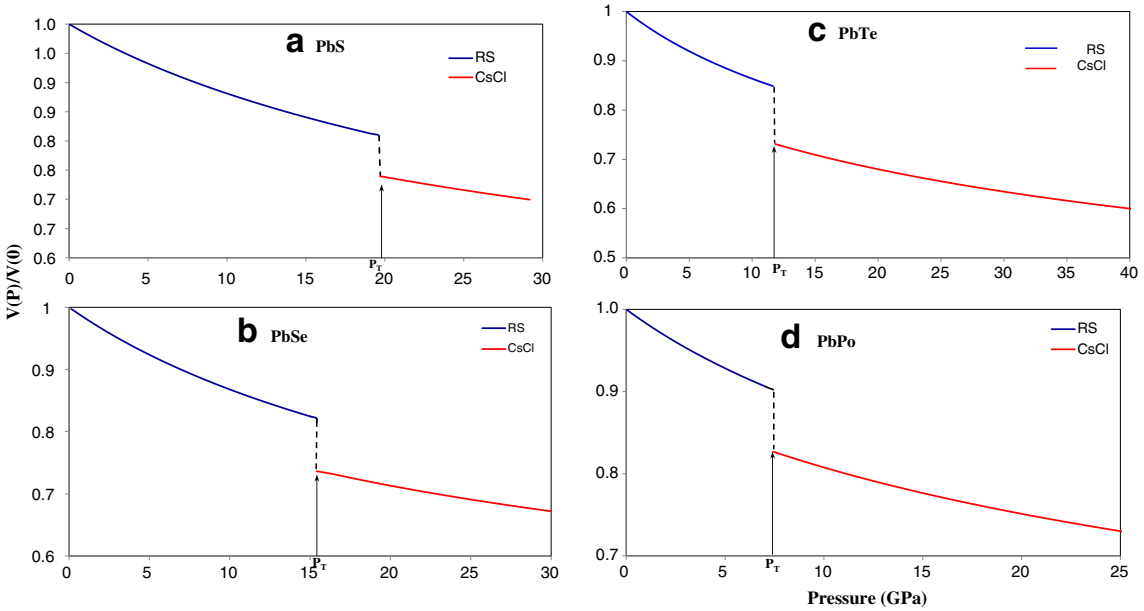

Fig. 3 Equation of state for lead chalcogenides

Table 2 Values of elastic constants (in GPa) and other properties for RS phase

Solids	C_{11}	C_{12}	C_{44}	C_S	B	C_L	G	ξ	A	P	Y	σ	B/G	References
PbS	137.50	23.50	19.60	57.00	61.50	100.10	34.56	0.32	0.34	1.95	87.32	0.26	0.56	Present
	124	33	23	–	–	–	–	–	–	–	–	–	–	Expt.[21]
PbSe	114.50	16.00	16.90	49.25	48.83	82.15	29.84	0.29	0.34	−0.45	74.37	0.25	0.61	Present
	123.7	19.3	15.9	–	–	–	–	–	–	–	–	–	–	Expt.[21]
PbTe	121.10	5.40	10.60	57.85	43.97	73.85	29.50	0.19	0.18	−2.60	72.32	0.23	0.67	Present
	105.3	7.0	13.2	–	–	–	–	–	–	–	–	–	–	Expt.[21]
PbPo	84.63	2.10	5.40	41.27	29.61	48.77	19.75	0.17	0.13	−1.65	48.46	0.23	0.67	Present
	–	–	–	–	–	–	–	–	–	–	–	–	–	Expt.[21]

The optimized values have been used to compute the crystal properties of present set of materials.

Results and discussion

The full structural optimizations, allowing simultaneous variations of unit cells and atomic positions, were performed and plotted in Fig. 1(a–d) for PbX in RS and CsCl structures, together with the information concerning the static equation of state (EOS) and the phase stability data. By exploiting the curves of minimization, it is found that the most stable phase at zero pressure is B1, which has lowest total energy as compared to CsCl structure for all materials.

The equilibrium lattice parameter, bulk modulus and its first-order pressure derivative along with total energy of PbX compounds in both the phases have been presented in Table 1. It shows that our calculated values for the RS phase are in agreement with experimental and theoretical [21, 22] values. The trend of E–V curves in Fig. 1(a–d) suggests the occurrence of phase transition from the NaCl to the CsCl structure under compression in each material. As is known, at zero temperature, the thermodynamically stable structure under hydrostatic pressure (P) can be obtained with the lowest enthalpy, H=E–PV. Therefore, the static transition pressures (P_T) between the RS and CsCl structures of PbX compounds can be estimated from the usual condition of equal enthalpies, i.e., $H_{RS}(P_T)=H_{CsCl}(P_T)$. Figure 2(a–d) displays the enthalpy as a function of pressure in B1 and B2 phases for all materials under consideration. It may be seen from these figures that PbX (X=S, Se, Te, Po) compounds undergo a pressure-induced phase transition from RS to CsCl structure at 19.4, 15.5, 11.5 and 7.3 GPa, respectively. The values obtained in the present case are in closer agreement with the available values [15–23].

The variation of reduced volume (V(P)/V(0)) with pressure has been plotted in Fig. 3(a–d) to get the equation of state (EOS) and understand the mechanism of transformation in these materials. It is clear from this figure that the volume of these compounds decreases smoothly up to P_T. At P_T, an abrupt change in volume is observed, which is associated with first-order structural transformation from B1→B2 phase along with the percentage volume collapse of 7 %, 9 %, 12 % and 8 %, respectively.

The elastic properties of a solid define the strength and compressibility of a material under the exerted amount of external pressure and its ability to return to the original or near original state after force is removed, and hence play an important role in providing valuable information about the binding characteristics between adjacent planes of atoms. On the basis of elastic properties, anisotropic character of binding and structural stability can also be predicted. In the present study, due to cubic symmetry the materials have only three independent elastic parameters (C_{11}, C_{12} and C_{44}), which along with their combinations are calculated and listed in Table 2.

Table 3 The calculated values of longitudinal, transverse and average sound velocities (νl, ν_t and ν_m in m/s) and Debye temperature (θ_D in K) for lead-chalcogenides in B1 phase

Solids	ν_l	ν_t	ν_m	θ_D in K (present)	θ_D in K (others)
PbS	3988.15	2313.19	2567.03	251.37	222.2 (ref. 30)
PbSe	3366.00	1953.21	2167.46	190.17	199.1 (ref. 30)
PbTe	3148.54	1873.69	2074.39	192.37	175.1 (ref. 29)
PbPo	2352.05	1397.44	1547.36	141.95	–

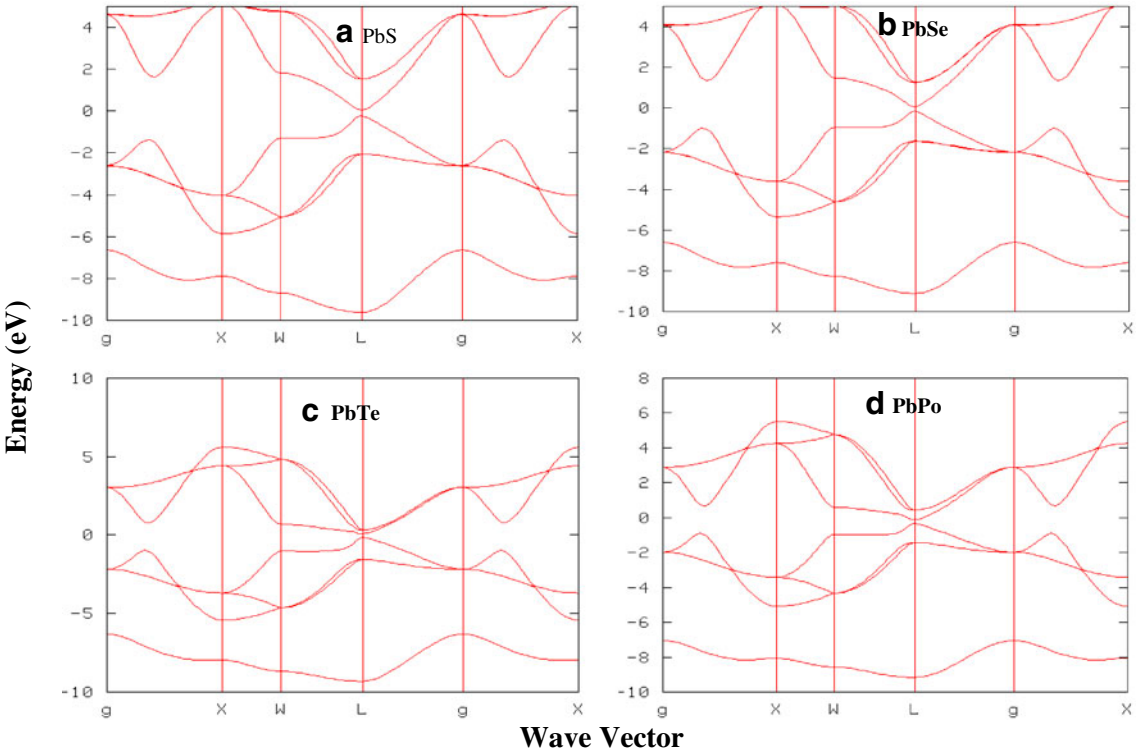

Fig. 4 Band structure of Pb-chalcogenides in rock-salt phase (Fermi level is set to zero)

It is clear from this table that the unidirectional elastic constant C_{11}, which is related to the unidirectional compression along the principal crystallographic direction, is higher than C_{44} in every case. This indicates that these materials present a weaker resistance to the pure shear deformation compared to the resistance to the unidirectional compression.

For cubic crystal structure the necessary condition of existence in a stable or meta-stable phase depends upon certain relationships of its elastic constants. The mechanical stability criteria [24, 25]

$$C_{11} > 0; C_{12} > 0; C_{11}{-}C_{12} > 0; C_{11} + 2C_{12} > 0 \quad (3)$$

is satisfied well in lead-chalcogenides and hence these materials are mechanically stable in B1 phase.

The elastic anisotropy [26] of crystals which is given by

$$A = \frac{2C_{44}}{C_{11}{-}C12} \quad (4)$$

Table 4 Calculated values of band gaps for RS phase (Fermi level is set to zero)

Solids	Present work	Expt. [23]	Others [22]
PbS	0.28	0.29	0.26
PbSe	0.18	0.17	0.16
PbTe	0.19	0.19	0.17

has an important implication in engineering science, to study the possibility to induce micro-cracks in the materials [27]. For an isotropic material, A is equal to 1, otherwise the material is anisotropic. The magnitude of the deviation from 1 is the measure of the degree of elastic anisotropy. The calculated values of A for lead-chalcogenides are listed in Table 2 and it shows that these materials are anisotropic in nature. We have calculated other important elastic constants viz, Poisson's ratio, Shear and Young's moduli.

Shear modulus of a crystal is the measure of the resistance to reversible deformation upon shear stress and it is an important factor to predict the hardness rather than bulk modulus. Another quantity to characterize materials is Young's modulus Y. The materials with higher value of Y are stiffer than those with lower Y values. Hence, on the basis of the present study, we can conclude that the stiffness of lead-chalcogenides decrease when we move from S to Po.

There are many other factors which are very useful to investigate the ductile and brittle nature of materials as Cauchy's pressure, which is given as

$$C_{12}{-}C_{44} = 2P \quad (5)$$

and Pugh's index of ductility which is the ratio of G and B, where

$$G = \frac{C_{11}{-}C_{12}{-}3C_{44}}{5} \quad (6)$$

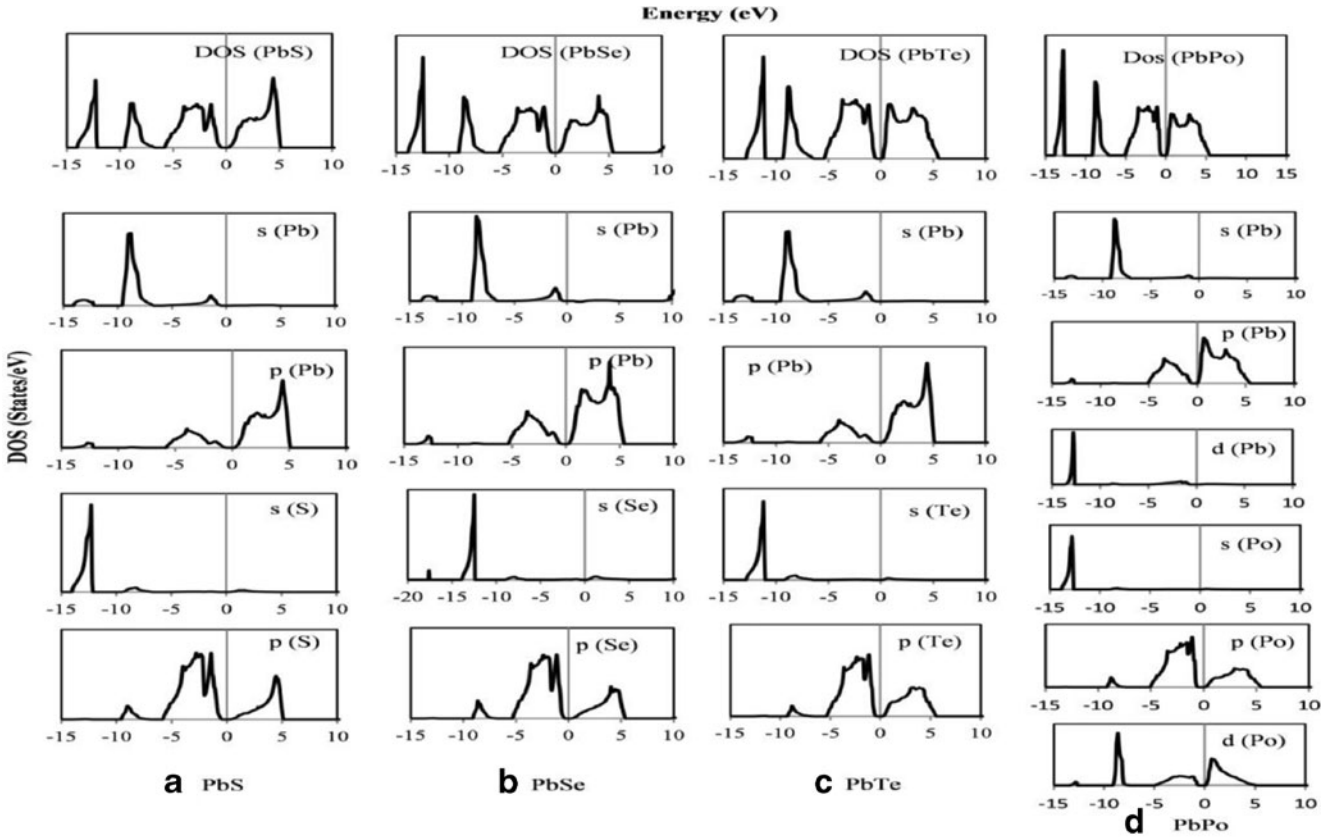

Fig. 5 PDOS and DOS of Pb-chalcogenides in rock-salt phase

Cauchy's pressure is the difference between two particular elastic constants ($C_{12} - C_{44}$) and is one of indicators of ductility [28]. The material with positive pressure is ductile and if the pressure is negative, brittle nature of the material is expected. In case of lead-chalcogenides PbS has positive value of pressure and

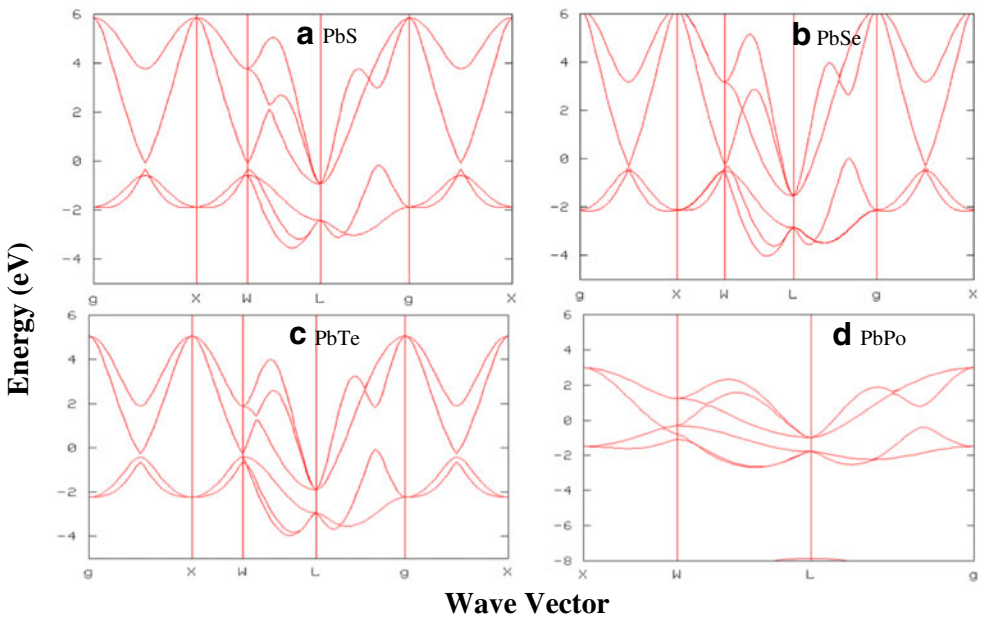

Fig. 6 Band structure of lead chalcogenides in CsCl phase

hence the material is expected to be ductile, while other lead-chalcogenides are brittle due to negative pressure as reported in Table 2.

The high G to B ratio is associated with brittle nature while low value shows ductile nature of material [29]. The critical number which separates the ductile and brittle nature is 0.57. We can classify the materials accordingly from the deviation of 0.57. As predicted from Cauchy's pressure, Pugh's index of ductility also predicts the ductile nature of PbS in the present study in B1 phase and the rest of the materials are expected to behave as brittle.

To study the thermal properties, we have calculated the Debye temperature θ_D for lead-chalcogenides using

$$\theta_D = \frac{h}{k_B}[3n/4\pi V_a]^{1/3}\nu_m \tag{7}$$

where the constants have their usual meanings. Here, V_a is atomic volume while average speed of sound (ν_m) in the polycrystalline material is given as

$$\nu_m = \left[(1/3)\left((2/\nu_t^3) + (1/\nu_l^3)\right)\right]^{-1/3} \tag{8}$$

with ν_l and ν_t as the longitudinal and transverse sound velocities, obtained by using elastic constants.

The calculated sound velocities and Debye temperature for present materials are reported in Table 3 along with other experimental and theoretical values. The slightly higher value of θ_D in the case of PbTe may be due to the fact that density value for PbTe is more (8.4 gm/cm^3) than the experimental (8.2 gm/cm^3) value. However in the case of PbS and PbSe the present results are close to the earlier theoretical [30] results.

As shown in Table 1, the equilibrium lattice constant is quite close to the experimental values. We have calculated the electronic structure of the present set of materials at computed lattice constants. The band gap is located at L point of the Brillouin zone as shown in Fig. 4(a–d). For the width of the band gap and overall ordering of bands, the present study shows closer agreement with the experimental data [23] as mentioned in Table 4 and better than earlier calculated values [1, 31] for PbS, PbSe and PbTe.

Figure 4(d) shows band structure of PbPo, the main feature of the band structure is that the valence band maximum and the conduction band minimum occurs at L point of the Brillouin zone as found for other compounds of this family. Unlike other PbX compounds, PbPo is semimetal as established earlier [32, 33]. In order to understand the contribution to the electronic structure of these compounds, we have computed total and partial density of states (DOS and PDOS) as shown in Fig. 5(a–d). It is seen that in each compound the bands just below the Fermi level (E_F) are predominately p states of chalcogen atom with a small contribution from 6p of Pb. The lowest bands have exclusively chalcogen atom s character, while the next bands are due to the s orbitals of Pb and lie far below the gap. The conduction band originates mainly out of p orbitals of Pb in PbS, PbSe and PbTe while PbPo shows small contribution of the d states of Pb and Po along with p of Pb.

To study the mechanism of transition, we have also investigated the electronic structure at high pressures in CsCl phase. It is found that these materials show metallization under pressure. The band structure of PbX in high-pressure B2 phase is reported in Fig. 6 (a–d).

In order to understand the pressure dependence of band gap of these materials, we have also studied the electronic structure of these compounds near the transition pressure in B1 phase. The results are shown in Fig. 7(a–c). It is clear from these figures that with increasing pressure, the conduction band minimum further approaches toward Fermi level. However, in B2 phase, no gap is observed, showing metallization. The

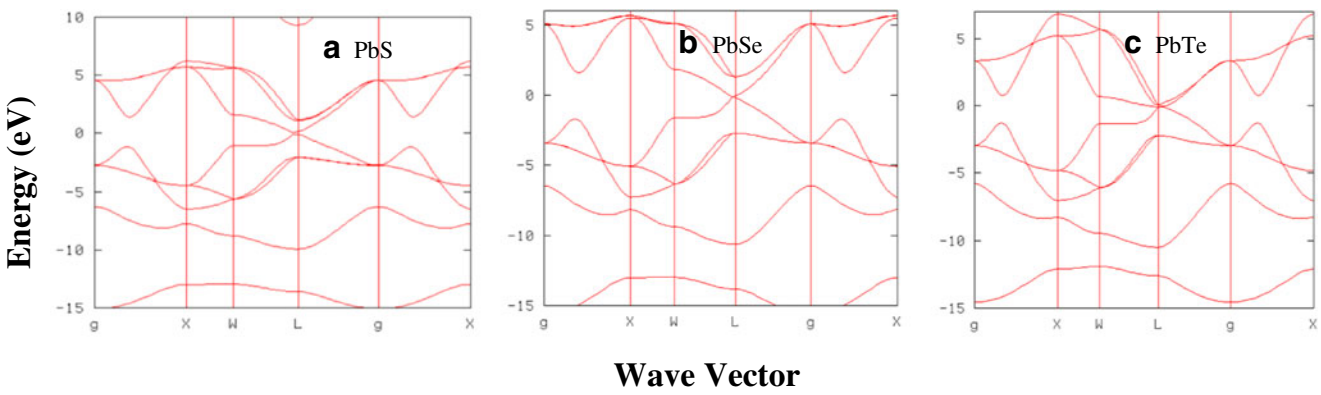

Fig. 7 Band structure of lead chalcogenides near P_T in B1 phase

pressure dependence of band gap energies is plotted in Fig. 8(a–c). It is found that the absolute conduction band minimum does not change its location in the BZ and remains at *L*-point. It is seen that the band gap increases linearly with pressure at *X*, *W* and *Γ* points of the BZ, however, it decreases with pressure at *L* point. It can be concluded from pressure variation of band structure that metallization occurs at *L* point in these compounds. It is also seen from Fig. 8(c) that the gap at *W* increases more rapidly than at *Γ* and makes a crossover at 8 GPa in PbTe.

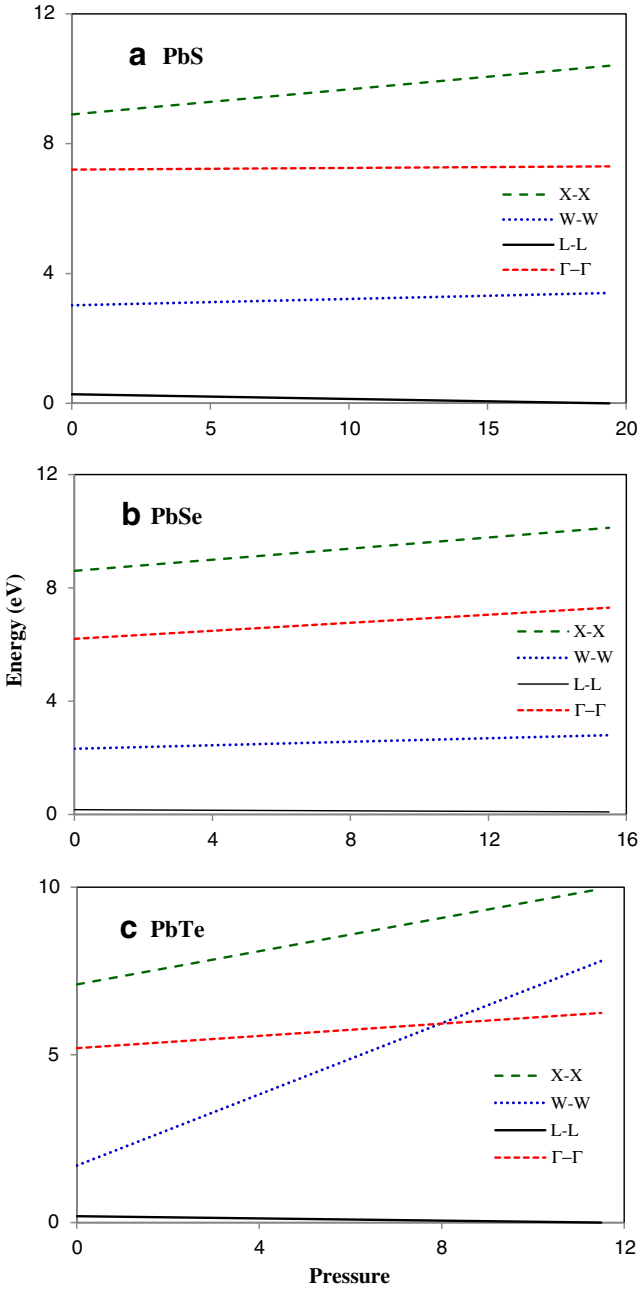

Fig. 8 Variation of band gap energies with pressure

Conclusions

We have studied the electronic band structure, elastic and phase transition properties of the lead chalcogenides (PbS, PbSe, PbTe, PbPo) from ab-initio self-consistent calculations based on fully relativistic pseudo-potential method. The present results show that the equilibrium lattice constants are in good agreement with experimental and other theoretical data. In general, our values of the mechanical properties of these compounds in the RS phase give the correct prediction of the experimentally observed values. In addition, we found that unlike other lead chalcogenides, PbPo is semi-metal in the parent (RS) phase. We have also found the phase transition in lead chalcogenides and the energy gap between conduction band and valence band varies with pressure. At ambient pressure, they are semiconducting, with increase in pressure, semiconducting behavior starts disappearing and dominance of metallic behavior eventually is observed at high-pressures.

Acknowledgments The authors are thankful to University Grants Commission (UGC), New Delhi for financial support.

References

1. Nabi Z, Abbar B, Mecabih S, Khalfi A, Amrane N (2000) Comput Math Sci 18:127–131
2. Samara GA (1983) Phys Rev B27:3494–3505
3. Welber B, Cardona M, Kim CK, Rodriguez S (1975) Phys Rev B12:5729–5738
4. Chaudhuri TK (1992) Int J Eng Res 16:481–487
5. Preier H (1979) Appl Phys 20:189–206
6. Zogg H, Alchalabi K, Zimin D, Kellermann K (2003) IEEE Trans Electron Devices 50:209–214
7. Moore GE (1965) Philosophical studies. Routledge
8. Findlay PC, Pidgeon CR, Kotitschke R, Hollingworth A, Murdin BN, Langerak CJGM, van der Meer AFG, Ciesla CM, Oswald J, Homer A, Springholz G, Bauer G (1998) Phys Rev B58:12908–12915
9. Rogalski A (1995) Infrared photon detectors. SPIE Optical Engineering Press, Washington
10. Maclean J, Hatton PD, Piltz RO, Grain J, Cernik RJ (1995) Nucl Instrum Methods Phys Res B97:354–357
11. Onodera A, Fujii Y, Sugai S (1986) Physica BC139/140:240–245
12. Chattopadhyay T, Von Schnering HG, Grosshans WA, Holzapfel WB (1986) Physica B139/140:356–360
13. Fujii Y, Kitamura K, Onodera A, Yamada Y (1984) Solid State Commun 49:135–139
14. Ferhat M, Zaoui A, Certier M, Khelifa B (1996) Phys Lett A216:187–190
15. Singh RK, Gupta DC, Sanyal SP (1988) Phys Stat Sol (b) 149:121–125
16. Bencherif Y, Boukra A, Ferhat M, Zaoui A (2012) Physica B:3520–3523
17. Hohenberg P, Kohn W (1964) Phys Rev B136:864–871
18. Kohn W, Sham LJ (1965) Phys Rev A140:1133–1139
19. Ceperley DM, Alder BJ (1980) Phys Rev Lett 45:566–569
20. http://www.openmx-square.org

21. Madelung O, Schulz M, Weiss H (Eds) (1983) Numerical data and functional relationships in science and technology Landolt-Bornstei. New Series vol. 17 Springer, Berlin
22. Hummer K, Gruneis A, Kresse G (2007) Phys Rev B75:195211–195219
23. Dornhaus R, Nimtz G, Schlicht B (1985) Narrow-gap semiconductors. Springer, Berlin
24. Mehl MJ, Osburn JE, Papaconstantopoulous DA, Klein BM (1990) Phys Rev B41:10311–10323
25. Mehl MJ (1993) Phys Rev B47:2493–2500
26. Hill R (1952) Proc Phys Soc London A65:349–354
27. Tvergaard V, Hutchinson JW (1988) J Am Ceram Soc 71:157–166
28. Pettifor DG (1992) Mater Sci Technol 8:345–349
29. Pugh SF (1954) Phil Mag 45:823–843
30. Labidi M, Labidi S, Hassan F (2012) ScienceJet 1(2):1–4
31. Wei SH, Zunger A (1997) Phys Rev B55:13605–13610
32. Rabii S, Lasseter RH (1974) Phys Rev Lett 33:703–705
33. Baleva M, Mateeva E (1994) Phys Rev B50:8893–8896